

Research Journal of Pharmaceutical, Biological and Chemical Sciences

Preparation of mono, di, and tri- activated carbon based Composites For Kerosene Desulfurization in Slurry Bubble Column Reactor.

Nada S Ahmedzeki^{1*}, Salah M Ali², and Sarah R Al-Karkhi¹.

¹Chemical Engineering Department, Baghdad University, Baghdad, Iraq.

²Petroleum Research and Development Center, Baghdad, Iraq.

ABSTRACT

In the present work, the catalytic oxidation desulfurization of Iraqi kerosene with sulfur content 2850 ppm was examined in a semi batch slurry bubble reactor at ambient conditions with oxygen gas, as the oxidant, and by using different metal oxides loaded on activated carbon to improve the chemical properties of the surface. The physicochemical properties for these adsorbents were characterized using X-Ray Diffraction (XRD), X-Ray fluorescence (XRF), N₂ adsorption for BET surface area, pore volume and Atomic Force Microscopy (AFM). Metal oxides loaded on activated carbon prepared by thermal co-precipitation method. Different factors such as type of the composite ZnO/AC, ZnO/NiO/AC and ZnO/NiO/CoO/AC, composite loading of 10, 15 and 25 g/l, flow rate of oxygen of 4.762, 9.524 and 19.048 l/min, and reaction time of 30, 45 and 60 min were studied. Results were analyzed by the Taguchi method in order to find the best conditions for desulfurization by slurry bubble column. The tri composite of ZnO/NiO/CoO/AC got the highest average sulfur removal of about 36%, and the sulfur removal at the best condition was 39% for kerosene, and 43% for model fuel with sulfur content of 2250 ppm at 55 min. The system for the model synthetic fuel was best fitted by a pseudo second order kinetic model at the best conditions. The effect of superficial gas velocity on gas hold up is investigated. The calculated Thiele modulus values at different composite type, assured that the effect of internal mass transfer could be neglected.

Keywords: Oxidation desulfurization; Slurry Bubble Column; Kerosene; Taguchi method; Activated carbon loaded; Oxygen Gas

**Corresponding author*

INTRODUCTION

Sulfur present in fuels leads to SO_x air pollution generated by vehicle engines [1]. These gases react with water in the atmosphere to form sulfates and acid rain which damage buildings, affect the paints of vehicles, occasioned an acid in a soil, as results lead to loss of forests and various other environmental systems[2]. Traces of sulfur present in fuels also poison the catalyst that is used in refining and cracking and cause premature breakdown of combustion engine and reduce the effectiveness for the oxidation of harmful carbon monoxide, hydrocarbons and volatile organic matter [3]. Sulfur emissions are a source of different human health problems and contribute to formation of atmospheric particulates, water pollution and global warming [2]. Also sulfur needs to be removed from the petroleum fractions as it causes corrosion of downstream refining equipment due to its acidic nature. The specifications of transportation fuels are changing significantly on worldwide, as shown in Table 1.

Table 1: Reduction of Sulfur content from different type of fuels

| Fuel Type | Sulfur Content | Reference |
|-----------|------------------------|-----------|
| Gasoline | 150 ppm (2001) | [4] |
| | 50 ppm (2003) | [5] |
| | 30 ppm (2006) | [6] |
| | 10 ppm (2009) | |
| Fuel oil | 2000 ppm | [7] |
| | Less than 15 ppm | [6] |
| Diesel | 2000 to 500 ppm (1997) | [1] |
| | 50 ppm (2005) | [8] |
| | 10 or 15 ppm (2009) | [9] |

The main desulfurization methods are the Hydrodesulfurization(HDS) and non- HDS such as; extraction, adsorption, oxidation and combination of these processes with HDS to reduce the consumption of H₂. HDS process needs high temperature (>257°C) 270-330°C and high pressure range (30-80 bar) by reacting hydrogen gas with sulfur compounds in the presence of catalyst [10].

ODS can be used instead of HDS due to mild conditions, lower temperature range (40-100°C) and lower pressure range(1- 2bar)[9].Also, performing this process at room temperature and atmospheric pressure, made it economic and novel, since the refractory sulfur compounds which are not removed in HDS process can be oxidized to sulfones that can be removed by adsorption and/or extraction [8]. The recovery of hydrocarbons from sulfones generated by ODS, enhances the desirability of using ODS for oil refining compared to the HDS [10].

Refractory sulfur compounds (like DBT and alkyl DBTs) require severe conditions in HDS process, because of the steric hindrance of alkyl group that makes the difficulty to interact with solid catalyst. But the situation in ODS is reverse to HDS. The presence of alkyl group in sulfur compounds increases the reactivity of the process due to the electronic effects, since the alkyl group is increasing the electron density around the sulfur atom by giving the electron [8].

Oxidation desulfurization can use direct peroxide or other liquid oxidant or it may generate peroxide in situ by the oxidation hydrocarbon, aldehyde or alcohol.

Most previous studies in oxidation desulfurization have concentrated on the use of hydrogen peroxide as the oxidant. Although ODS with peroxides is attractive because the reaction conditions are mild, the large scale of employing and storage of peroxides are quite dangerous and costly. For the process to be feasible, the oxidant must be inexpensive. The most economical oxidizer on an industrial scale is oxygen gas.

There has been some work to generate the peroxide species in-situ as follows:

1. Using Oxygen gas, air [7] and ozone [11]
2. Oxidation of an aldehyde (octanal), with a metal salt as catalyst [1] or without metal salts [8].

3. Oxidation of alcohol (2- propanol) [12].
4. Reaction of oxygen gas with hydrogen.

In case of using oxygen gas, there are two possible ways to oxidize sulfur containing compounds to the corresponding sulfones; direct and indirect use of oxygen. The direct use of oxygen is suitable for treating mercaptans and is usually carried out in basic solution such as sodium hydroxide or ammonia with the use of sulfonated cobalt phthalocyanine as catalyst in a process called Merox process [13]. In the indirect oxidation process, oxygen carrier molecules are used, which can selectively oxidize sulfur. The oxygen carrier can be used with regeneration or without regeneration. For regenerable oxygen carrier, the sulfur containing compounds are oxidized in two steps: first, is the oxidation of sulfur containing compounds by the oxidizer such as nitrogen oxide (NO). The second step is the regeneration of the oxidizer by using molecular oxygen [14]. In case no regeneration is employed, oxygen is transferred to a carrier (solvent) to form a hydroperoxide, followed by the reaction of hydroperoxide with sulfur compounds to form sulfones [6]. A chain-radical mechanism suggested the initiation step where the hydrocarbon is oxidized to form radical. The radical is reacted with molecular oxygen in propagation step, to form the hydroperoxide radical, then hydroperoxide radical reacts with another molecular of hydrocarbon to give a peracid and regenerate the another radical. The peroxyacid oxidizes the sulfur heterocycle twice to give a sulfone [6].

Sherman, 2001 presents the oxidation with sub-micron size bubbles (sintered glass, sintered ceramic, or porous ceramic tube for generate sub-micron bubbles of ozone for desulfurization of diesel fuel) [15]. Ma et al., 2007 studied ODS of a model jet fuel (BT, 2-MBT, 5-MBT and DBT dissolved in n-Decane) with sulfur content 412 ppm being reduced to 2 ppm and a real jet fuel (JP-8) with sulfur content 717 ppm reduced to 126 ppm with molecular oxygen at ambient condition and an adsorption using Fe (III) nitrate and Fe (III) bromide with and without carbon support and also over an activated carbon. They founded that the oxidized sulfur compounds (sulfoxide and sulfone) are more efficient to be adsorbed than sulfide on surface of activated carbon due to the higher polarity of oxidized sulfur compounds and high electrostatic potential due to the increase of the dipole magnitude by the transfer of oxygen atom [16]. Imtiaz et al., 2013 studied ODS of model oil (thiophene, DBT, and 4-MDBT dissolved in n-heptane) with sulfur content 1275 ppm reduced to 57 ppm, and commercial oil (untreated naphtha, light gas oil, heavy gas oil and Athabasca) using an air-assisted performic acid oxidation with phase transfer catalyst (emulsion catalyst). The sulfur removal rate for commercial oil including untreated naphtha was 83%, light gas oil was 85%, heavy gas oil 68% and Athabasca 64% [17]. Wang et al., (2014) studied the extractive and oxidative desulfurization of BT, DBT and 4, 6-DMDBT dissolved in n-octane as model fuels with sulfur content 500 ppm in 70 ml autoclave at pressure of 0.3 MPa, temperature 80-140°C and 1 l/min oxygen flow rate using N-hydroxyphthalimide as a catalyst. Extraction by 1-butyl-3-methylimidazolium tetrafluoroborate [BMIM]BF₄ as an ionic liquid and oxidation by oxygen gas. The sulfur removal reached 100% with oxygen gas, and 32.9% with nitrogen gas (for flash out oxygen gas) and 51.6% with air [18]. Nawaf et al., 2015 studied ODS of DBT in light gas oil (LGO), initial sulfur content 1000 ppm, in trickle bed reactor with homemade manganese oxide (MnO₂/γ-Al₂O₃), the highest removal 81.2% (188 ppm) at 200°C [7]. Ding and Wang, 2015 studied ODS of DBT in n-octane as model fuel initial sulfur content 500 ppm, at mild conditions (1 atm and 90°C) using copper phosphotungstate (Cu_{1.5}PW₁₂O₄₀·15H₂O) as a catalyst, using air and oxygen as oxidant and distilled water as the solvent in extraction of sulfone after oxidation. The highest removal was 97% (15ppm) within 30 min at 800 ml/min oxygen gas. The comparison between oxidation of air and oxygen gas shows that the activities are close at same conditions. To ensure the actual oxygen feed rate 450 ml/ min air is equivalent to 90 ml/min oxygen gas which both reduce the sulfur to 130 ppm (74% removal) at 150 min [19].

The objective of present study is to introduce new technique for the reduction of sulfur compounds from Iraqi kerosene by using oxygen gas rather than hydrogen gas in slurry bubble column using different metal oxides loaded on activated carbon. The design of experiment by the Taguchi method was considered to find the best conditions. Slurry bubble column with reaction and without reaction systems is used in various chemical, petrochemical and biochemical applications, because of easy construction, low operating cost, simple use, cheap, and less repair and maintenance due to lack of moving parts, isothermal condition and high mass and heat transfer [20].

The desulfurization by using activated carbon is an effective and cheap method for removing sulfur compounds because of its porous structure having high surface area, large pore volume in addition to its

activity which can be used as adsorbent, catalyst and catalyst support [21]. Other useful common sorbents are transition metals, metal oxide, and molecular sieve, zeolites, and supported polymer[22].

The nature of activated carbon surface is hydrophobic; therefore a competitive adsorption can occur when subjected to treat fuels where it can attract other hydrocarbons like aromatics with the same cyclic structure. So, to enhance the selectivity of such adsorbents, the oxidation process to convert sulfides to sulfoxides and sulfones is adopted.

Also, loading with metal oxides; like silver, nickel, cobalt, copper, aluminum and iron was reported to increase the sulfur removal by reactive adsorption. This can be explained by π -interaction and acid-base interaction between metal species and sulfur compounds[23, 24, 25, 26].

The performance of incorporation of mixed metals oxides in the aforementioned past studies was studied for model fuels with low sulfur content and mainly in a batch mode of adsorption[27, 28, 29, 30]. The effect on a real fuel with different kind of hydrocarbons (paraffins, olefins, naphthenes, aromatics) can be quite different and the efficiency of the removal should be studied specifically for a certain petroleum fraction as a case study. In the present research, activated carbon was loaded with ZnO, NiO/ZnO and NiO/ZnO/CoO for investigation the reduction of sulfur compounds from both Iraqi kerosene and synthetic fuel using oxygen gas in a slurry bubble column reactor.

EXPERIMENTAL

Materials

All chemical compounds were of analar type. $\text{Zn}(\text{NO}_3)_2 \cdot 6\text{H}_2\text{O}$, 98% $\text{Ni}(\text{NO}_3)_2 \cdot 6\text{H}_2\text{O}$, 99.7%, $\text{Co}(\text{NO}_3)_2$, 99% NaOH, 99% , n-Nonane C_9H_{20} 99%, Dibenzothiophene $\text{C}_{12}\text{H}_8\text{S}$ 99% were supplied by Thomas Baker, India, Fisher certified, Panreac, Espana, Hopkin and Williams, England, BDH Chemicals, England, Himedia, India respectively. Iraqi Kerosene from the Midland Refineries Company/Al-Dura Refinery with sulfur content 2850 ppm. Activated carbon was from Thomas Baker/India.

Method of Preparing Composites

ZnO/AC and ZnO/NiO/AC composites were prepared by co-precipitation method [2]. In the present work, the new tri oxide composite of ZnO/NiO/CoO/AC was introduced by the same method.

Activated carbon was dried for one hour at 200°C before use. Water content was 72.74wt %. For loading zinc oxide, 10 g of activated carbon powder was dispersed in 250 ml deionized water so that to obtain the best dispersion. The solution of activated carbon and deionized water was mixed in a magnetic stirrer plate for 12 h. It was intended to obtain 10% loading (for single oxide or net mixed oxides). So, 1.8649 g of zinc nitrate hexahydrate was dissolved in 20 ml water. Then zinc nitrate solution was added drop wise to the dispersed activated carbon solution while stirring. The pH of the mixture was adjusted by adding 1M of NaOH solution until reaching 8. Heating the mixture was for 6 h at 90°C with reflux, followed by filtration, washing, drying overnight at 110°C and calcination the product for 3h at 250°C .

The di- composite ZnO/NiO/AC is prepared by similar steps as ZnO/AC. 0.9324 g and 0.97621g of zinc nitrate hexahydrated and nickel nitrate hexahydrate were used respectively to obtain \approx 5wt. % loading for each oxide. The tri- composite ZnO/NiO/CoO/AC is prepared by similar steps as AC/ZnO. 0.4917 g, 0.4917 g and 0.5382g of zinc nitrate hexahydrated, nickel nitrate hexahydrate and cobalt nitrate respectively to obtain \approx 3 wt. % loading for each oxide.

Characterization

The crystalline phase of zinc oxide, nickel oxide and cobalt oxide in the surface of activated carbon were studied by X-ray (XRD) using $\text{Cu K}\alpha$ radiation ($\lambda = 1.54056\text{\AA}$). XRD data within the 2θ range between 20° and 80° . The phase identification was accomplished by comparing with reference data from the International Center for Diffraction Data (ICDD). XRD analysis was performed on Bruker, D2 phaser (German 2010). The percent of each oxide in the prepared composite was done by X- ray Florescence (XRF) using Spectro XEPOS

(German 2010). Determination of prepared composite surface area and pore volume was achieved using BET method by Thermo Finnegan type, apparatus. BET surface area measurements were made by N₂ adsorption with the degassing temperature of 200°C for 1 h. Atomic Force Microscopy traces the topography of samples with extremely high resolution. (SPM-AT 3000 / Atomic force microscopy / Angstrom-Advance Inc., USA 2008 / contact model). The sulfur content of kerosene filtered was determined according to ASTM D-7039 by using the testing device (Sulfur analyzer, Sindie OTG, USA). UV-spectrophotometer instrument (Genesys 10 UV) was used to calculate the concentration of DBT in n-Nonane at 325nm wave length. Figure 1 shows the UV-calibration curve for concentration of DBT.

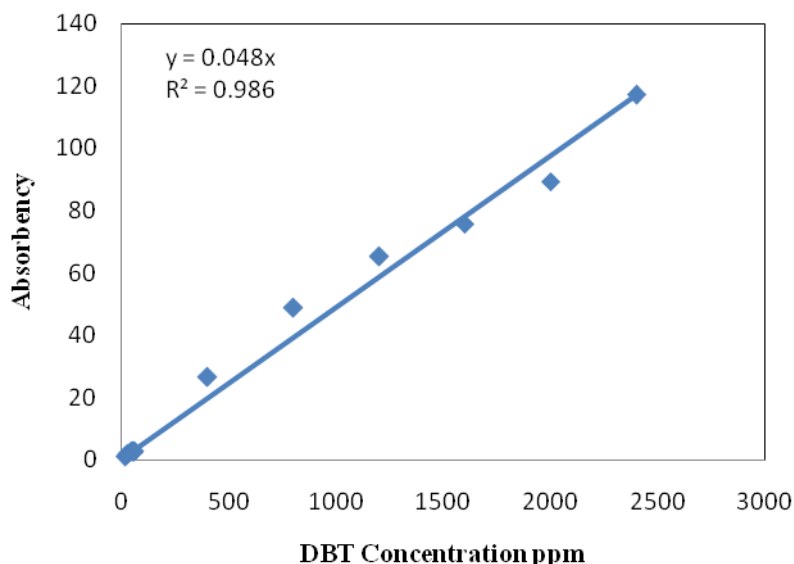


Fig 1: UV-calibration curve

Experimental Setup of Slurry Bubble Column Reactor (SBCR)

A bubble column reactor (QVF pyrexglass) of 7.6 cm outside diameter and 159 cm height was constructed for evaluating the activity of the prepared composites. Figure 2 shows a schematic diagram of experimental semi batch slurry bubble column. Different factors such as type of composite ZnO/AC, ZnO/NiO/AC and ZnO/NiO/CoO/AC, amount of composite 10, 15 and 25 g/l, flow rate of oxygen 4.7619, 9.5238 and 19.0476 l/min, and reaction time 30, 45 and 60 minutes have been studied in order to find the best conditions for desulfurization in slurry bubble column.

| Item No. | Description |
|----------|----------------------|
| 1 | Valve |
| 2 | Distributor |
| 3 | Slurry Bubble column |
| 4 | Conical Expander |
| 5 | Ball Valve |
| 6 | Needle Valve |
| 7 | Silica Gel Column |
| 8 | Rotameter |
| 9 | Pressure Gage |
| 10 | Oxygen Gas Cylinder |
| 11 | Manometer |

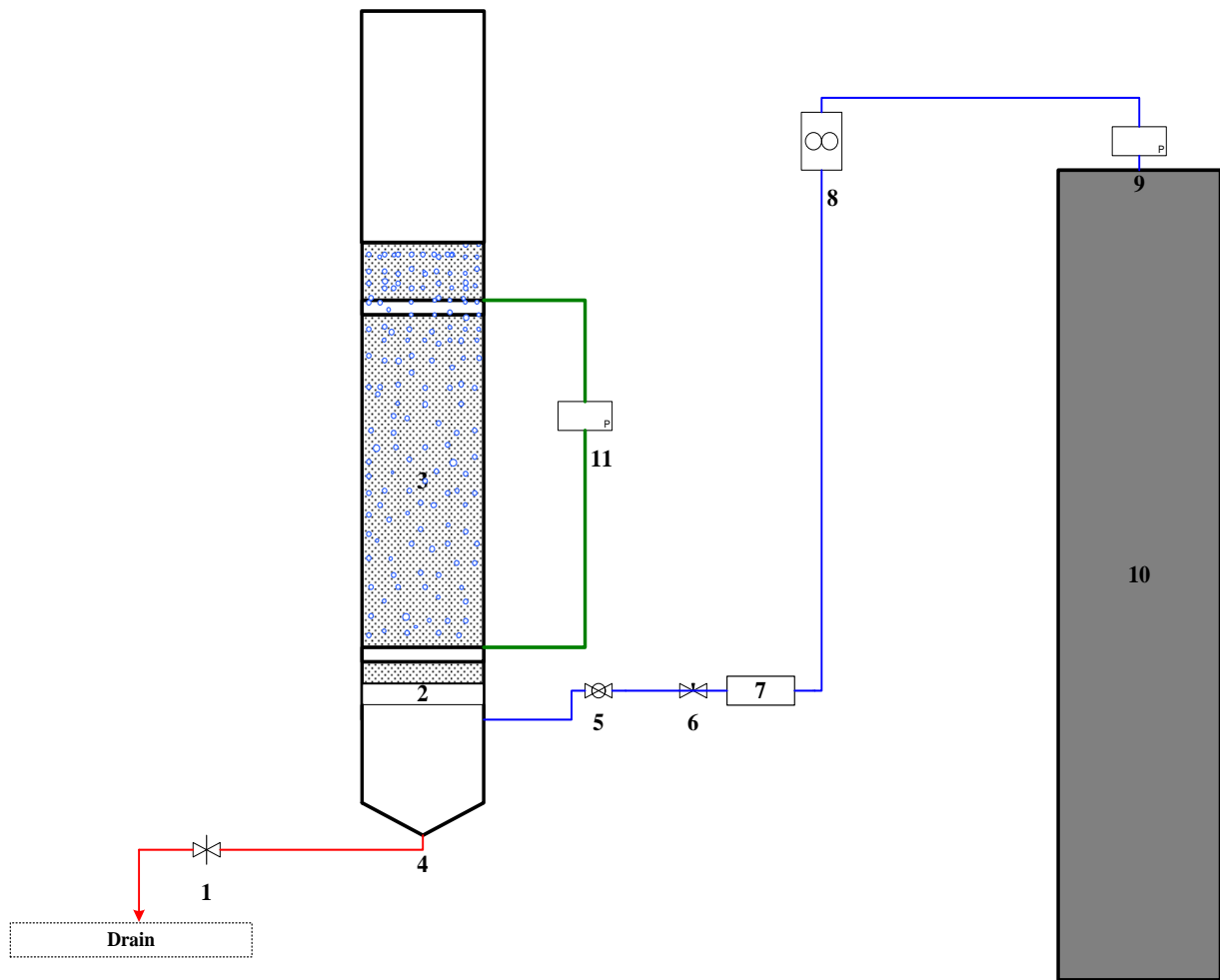


Fig 2: Schematic Diagram of SBCR

The perforated plate, made from Teflon, is used as the distributor. The perforated plate of 1 mm hole diameter with pitch of 5mm. The hole diameter of distributor was designed based on physical properties of kerosene and model fuel. The hole diameter of the distributor was calculated according to Ruff and Pilhofer 1978[31], as in Equation (1):

$$d_o = 2.32 \left[\frac{\sigma}{\rho_l g} \right]^{1/2} \left[\frac{\rho_l g}{\rho_l - \rho_g} \right]^{5/8} \dots (1)$$

The distributor was placed between the cylindrical section of the column and the reducer using two flanges equipped with gaskets. A rotameter was used for measuring the flow rate of air. The reading is corrected to convert to oxygen gas reading.

$$Q_{O_2} = \frac{Q_{air}}{1.05} \dots (2)$$

The correction factor air to Oxygen is 1/1.05 [32]. This correction factor is for density difference. Density of oxygen is 1.33035 kg/m³ (1atm and 20°C) is higher than air density 1.2056 kg/m³ (1atm and 20°C), thus, logically an oxygen gas in the tube will push the ball up lower than air. The pressure drop across SBCR is measured by a digital manometer. A digital manometer is installed to measure the pressure drop between 3cm and 80cm from gas distributor. The gas hold up in three phase slurry bubble column was determined based on the static height and dispersed height reading as in Equation (3).

$$\epsilon_g = \frac{H_d - H_0}{H_d} \dots (3)$$

Oxygen gas is passed through silica gel to remove the humidity. The flow rate was maintained at the desired value by the needle valve and rotameter.

RESULTS AND DISCUSSION

Characterization of the Composites

The XRD patterns of the parent activated carbon, showed the peaks between $2\theta = 20-30$ and $40-50$, which are noisy and disordered indicating the amorphous carbon as shown in Figure 3.

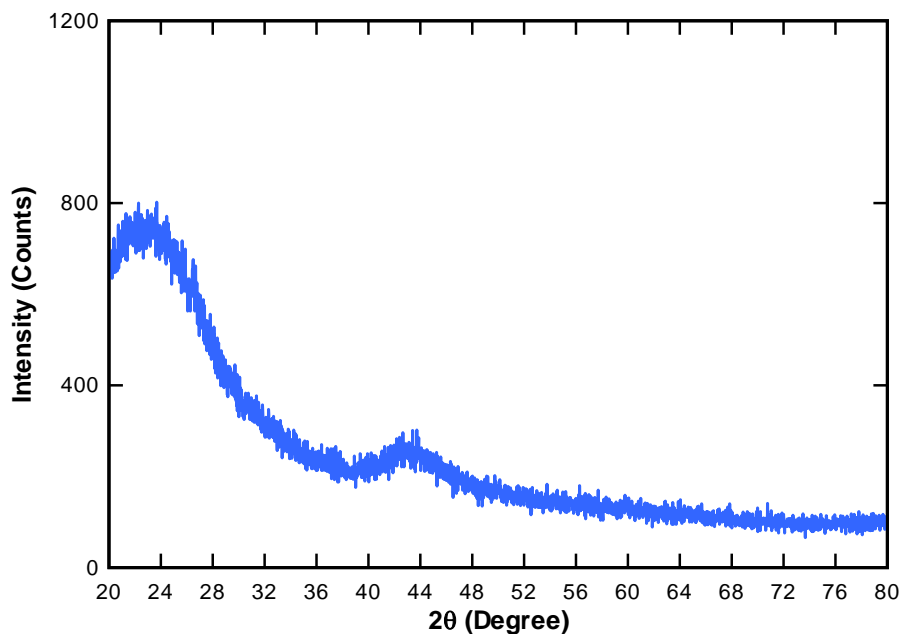


Fig 3: XRD Pattern of activated carbon

The XRD patterns of ZnO/AC, ZnO/NiO/AC, and ZnO/NiO/CoO/AC have new peaks existing in different 2θ and intensity of the original AC, as shown in Figures 4, 5, and 6. For ZnO/AC, the clear peaks at $2\theta = 34.438^\circ$, 36.249° and 47.539° as shown in Figure 4 indicates to the crystalline ZnO, and noisy background patterns indicate to amorphous carbon.

For ZnO/NiO/AC, the clear peaks at $2\theta = 31.748^\circ$, 34.438° , 36.249° , 47.539° , 67.912° , 69.052° , and 72.604° indicates to crystalline ZnO, and at $2\theta = 43.295^\circ$ refers to crystalline NiO, as shown in Figure 5.

For ZnO/NiO/CoO/AC, the clear peaks at $2\theta = 31.748^\circ$, 34.438° , 36.249° , 47.539° , 56.551° , 62.856° , 67.912° , 69.052° , 72.604° and 76.950° indicates to crystalline ZnO, and at $2\theta = 37.278$, 43.295 , 62.913 , $75,439$, and 79.387 indicate to crystalline NiO, and at $2\theta = 42.644^\circ$, 49.662° , 72.864° indicate to crystalline CoO as shown in Figure 6. The noisy background patterns in all aforementioned figures refer to amorphous carbon.

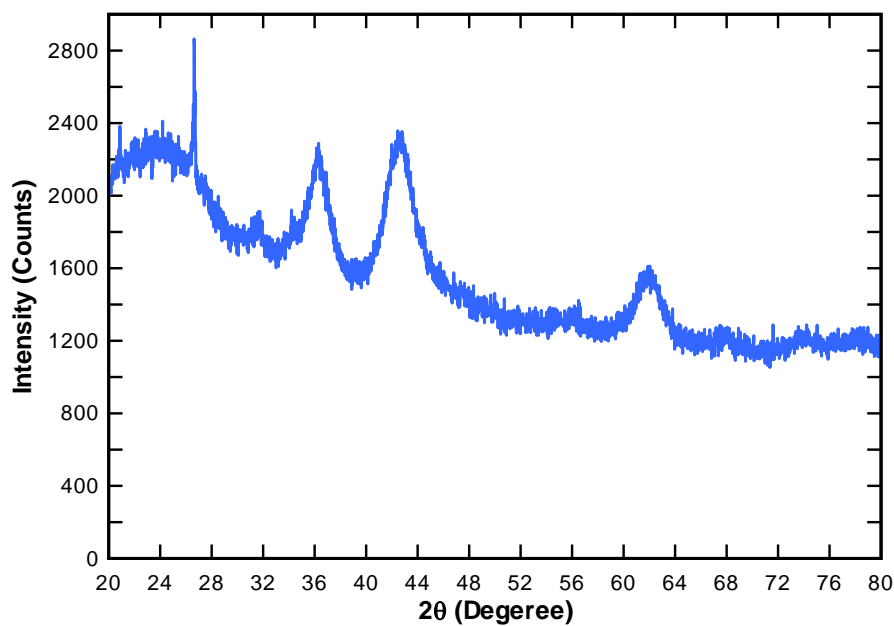


Fig 4: XRD Pattern of ZnO/AC

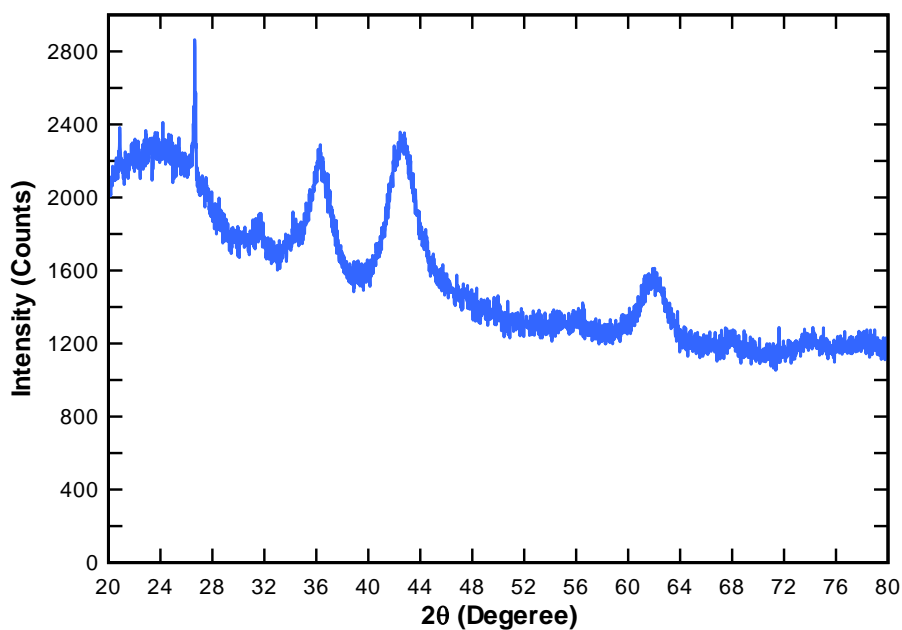


Fig 5: XRD Pattern of ZnO/NiO/AC

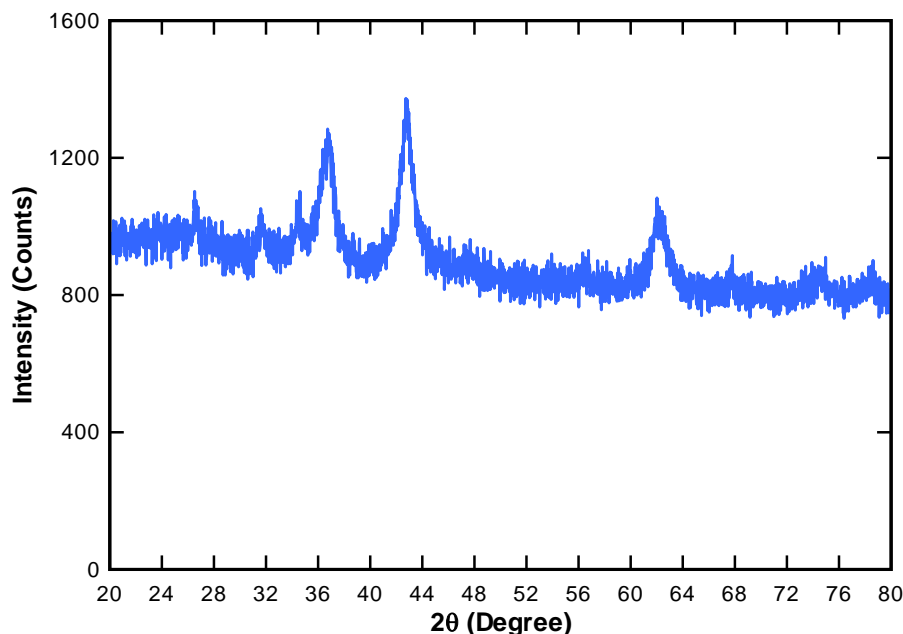


Fig 6: XRD Pattern of ZnO/NiO/CoO/AC

The XRF analysis shows the metal oxide composition for metals oxides loading on the surface of the activated carbon. A total measured metals oxides for each composite was ≈ 10 wt. %. The loading ratio was chosen 10wt % because the increasing in loading ratio causes the block of pore, and leads to decrease of surface area [33]. The oxide composition of the metals oxides loaded with activated carbon was obtained by XRF which is list in Table 2. It was found that the percentages of metals oxide in the activated carbon are close to the twice of theoretical percentages. This gives the indication that the activated carbon has higher oxygen content of oxygenated functional groups on the activated carbon surface in addition to other metal impurities as reported by Nazal 2015[25].

Table 2: XRF for Three Type Composites

| Composite Type | Metal oxide loaded | wt. % |
|----------------|--------------------|-------|
| ZnO/AC | ZnO | 10.73 |
| ZnO/NiO/AC | ZnO | 4.976 |
| | NiO | 4.851 |
| ZnO/NiO/CoO/AC | ZnO | 3.256 |
| | NiO | 3.072 |
| | CoO | 3.180 |

The surface area of the prepared composites was measured by BET method. Values of surfaces area and pore volume are listed in Table 3.

Table 3: Surface Area and Pore Volume

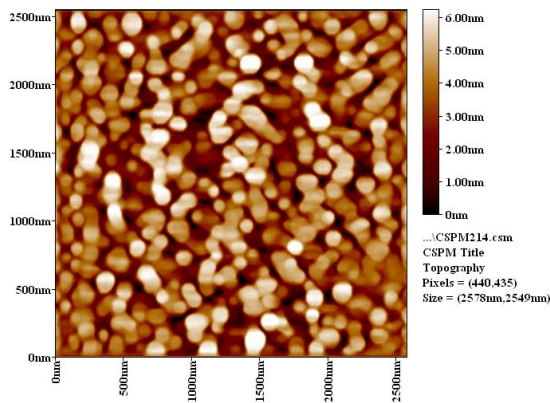
| | AC | ZnO/AC | ZnO/NiO/AC | ZnO/NiO/CoO/AC |
|-----------------------|-----------|--------|------------|----------------|
| Surface Area, m^2/g | 1005.5045 | 972.73 | 924.735 | 932.9787 |
| Pore Volume, cm^3/g | 0.6203 | 0.6114 | 0.6252 | 0.6031 |

There is a little decrease in surface area of activated carbon after loading of ≈ 10 wt % metals oxides as listed in Table 3. But, the surface area is still high and near from the values of original source, revealing a good

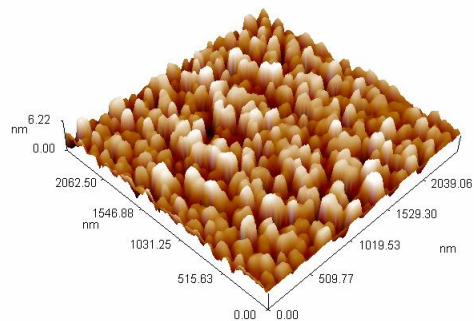
dispersion of the metals oxides [34].The increasing in particle size causes some decrease in the surface area. The average particles diameter was determined by AFM. Table 4 lists the particles size distribution of activated carbon and prepared composites. Figure 7 shows the topographical surface images of activated carbon and its composites in two dimensional (2D) and three dimensional (3D) were obtained from AFM analysis.

Table 4: Particle Size Distribution

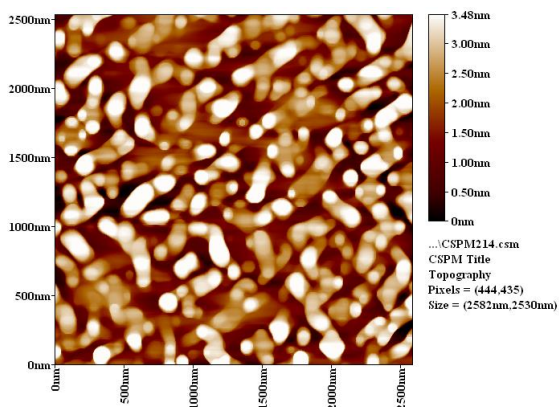
| Composite Type | Avg. Diameter nm | ≤ 10vol % nm | ≤ 50vol % nm | ≤ 90vol % nm |
|----------------|------------------|--------------|--------------|--------------|
| AC | 93.84 | 50 | 90 | 140 |
| ZnO/AC | 104.72 | 60 | 90 | 150 |
| ZnO/NiO/AC | 118.01 | 80 | 110 | 150 |
| ZnO/NiO/CoO/AC | 104.72 | 70 | 100 | 130 |



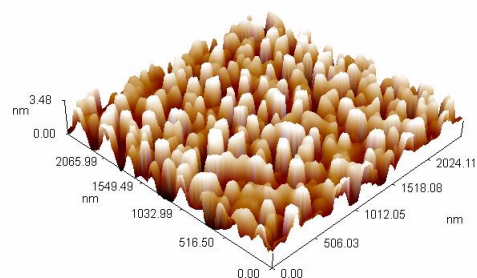
a) AC surface 2D



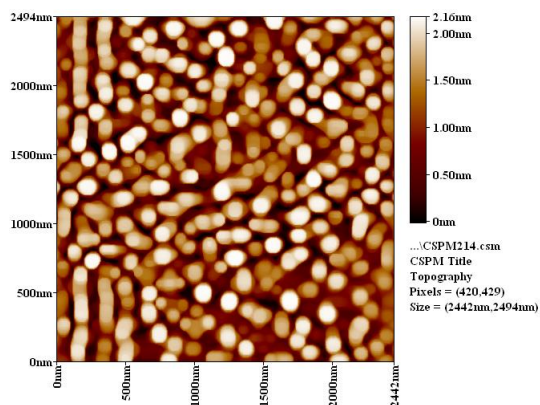
b) AC surface 3D



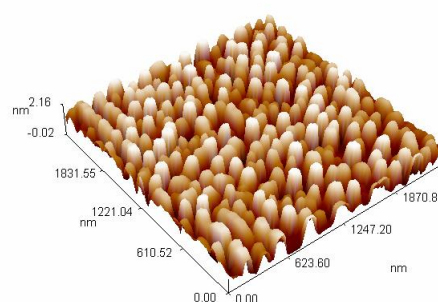
c) ZnO/AC surface 2D



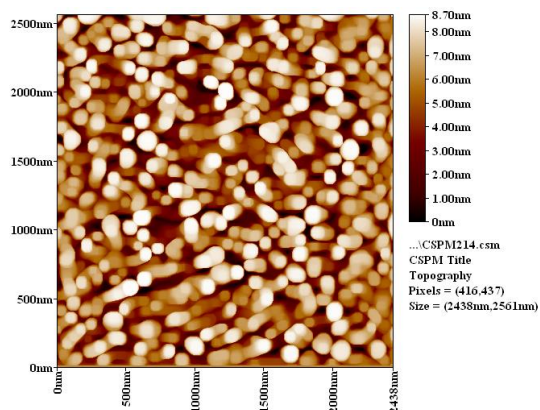
d) ZnO/AC surface 3D



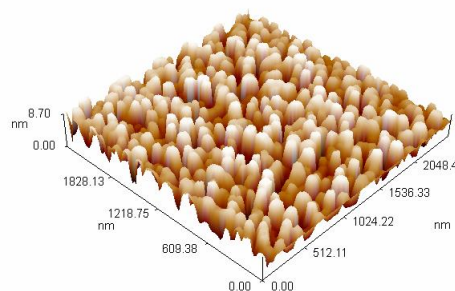
e) ZnO/NiO/AC surface 2D



f) ZnO/NiO/AC surface 3D



g) ZnO/NiO/CoO/AC surface 2D



h) ZnO/NiO/CoO/AC surface 3D

Fig 7: AFM of AC,ZnO/AC,ZnO/NiO/AC and ZnO/NiO/CoO/AC surfaces 2D and 3D

Oxidation Desulfurization of Kerosene

The experiments were carried out in a semi batch slurry bubble column. Oxygen gas was bubbled at different flow rates through the kerosene fuel. By Taguchi method, the results are statistically analyzed using the signal-to-noise (S/N) ratio to determine the best conditions and the percentage contribution of individual factors to the response (% sulfur removal). The results of % sulfur removal, factors and their level of the nine experimental runs are given in Table 5.

Table 5: % Sulfur Removal for each Experiment Run

| Exp. run | Factors and their Level | | | | % Removal |
|----------|-------------------------|-----------------------|---------------------------|-----------|-----------|
| | Composite Type | Composite Amount, g/l | Flow Rate of Oxygen l/min | Time, min | |
| 1 | ZnO/AC | 10 | 4.7619 | 30 | 22.8070 |
| 2 | ZnO/AC | 15 | 9.5238 | 45 | 27.3333 |

| | | | | | |
|---|----------------|----|---------|----|---------|
| 3 | ZnO/AC | 25 | 19.0476 | 60 | 29.8632 |
| 4 | ZnO/NiO/AC | 10 | 9.5238 | 60 | 31.8964 |
| 5 | ZnO/NiO/AC | 15 | 19.0476 | 30 | 32.4900 |
| 6 | ZnO/NiO/AC | 25 | 4.7619 | 45 | 37.5400 |
| 7 | ZnO/NiO/CoO/AC | 10 | 19.0476 | 45 | 35.8280 |
| 8 | ZnO/NiO/CoO/AC | 15 | 4.7619 | 60 | 32.3900 |
| 9 | ZnO/NiO/CoO/AC | 25 | 9.5238 | 30 | 38.5965 |

In Taguchi method, the signal to noise (S/N) ratio is employed to measure the quality characteristics deviating from the desired value, signal represent desired value and the noise represent the deviation from desire value. There are generally three kinds of S/N ratio "smaller-the-better", "larger- the-better" and "normal- the better". In the present study, "the larger is best" is considered and by using Minitab-17 software to analyze the results of Taguchi experimental design. Figure 8 shows the effect of four factors at different level on the main to S/N ratios.

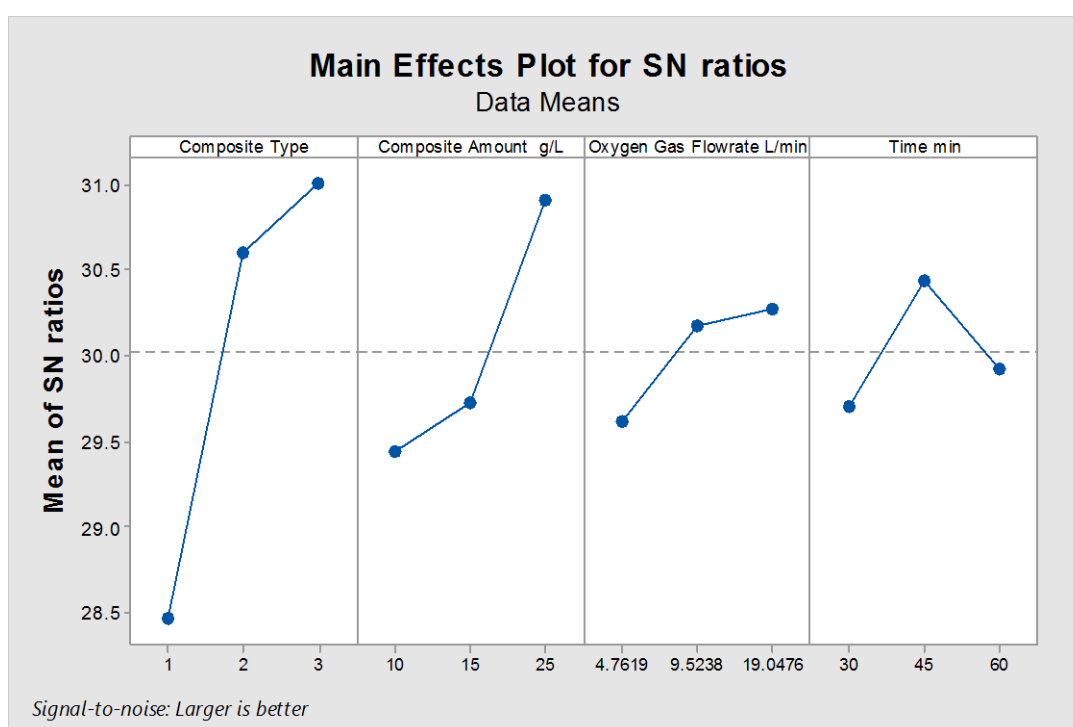


Fig 8: The effect of each factor at different level on the S/N ratio

The value of the maximum point of main S/N ratio indicates the best range of the experimental conditions. Therefore, the best conditions for the largest sulfur removal were composite type 3ZnO/NiO/CoO/AC at level 3, catalyst amount 25 g/l at level 3, oxygen gas flow rate 19.0476 l/min at level 3 and time 45 min at level 2. The sulfur removal at this best condition is about 39%.

The order of influence of the parameters in terms of the sulfur removal are composite type > composite amount > time > oxygen gas flow rate. Figure 9 shows the percent contribution of individual factors on variation in sulfur removal.

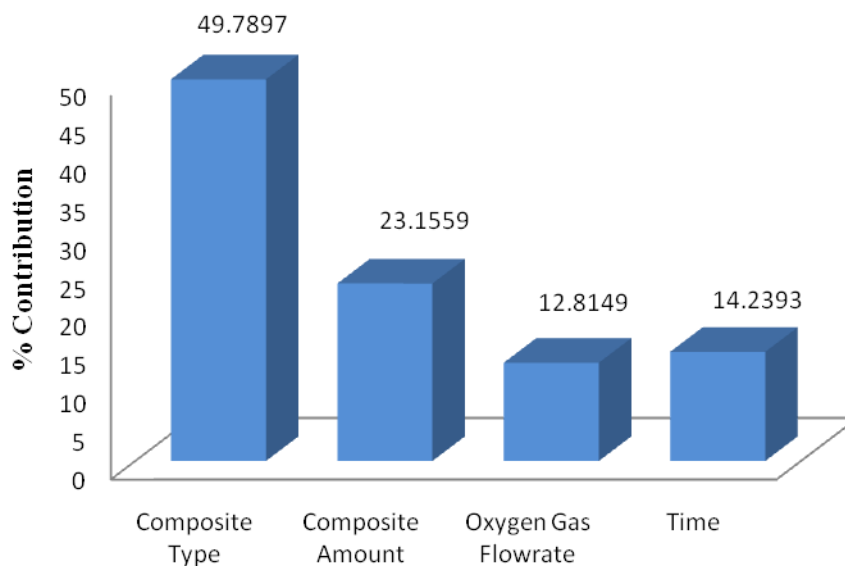


Fig 9: Percentage Contributions of Individual Factor

Analysis of the ODS in SBCR by the Taguchi method

For the nine experimental runs Table 5, the percent average of all the sulfur removal of a set of control factors at a given level was calculated from the effect of the factors and the interactions at specified levels. For example, in the case of composite type and level 1, the percent average sulfur removal (26.6678) was calculated using the values (22.8070, 27.3333 and 29.8632) from experiment runs 1, 2 and 3, and so on for all levels and factors.

Effect of Composite Type

The combination of tri metals oxides of ZnO, NiO and CoO was found to give the highest sulfur removal, where introducing cobalt oxide in the structure offered more suitable active sites for sulfone compounds. Figure 10 shows the main effect of composite type on sulfur removal. Results listed in Table 5.

These findings agree with past studies of reactive adsorption. Moosavi (2012) concluded that copper or nickel oxide loaded on activated carbon increased the sulfur removal from model fuel to 40-53% [24]. Alhooshani et al., (2015) used zinc oxide/activated carbon and zinc and nickel oxides/activated carbon composites for treating model fuel with sulfur content 190, 190 and 197 ppm for thiophene, BT and DBT respectively. The DBT gives the highest removal near 85% and for thiophene and BT near 40% and 45% respectively in 50 min for di composite. They concluded that the addition of di oxide exhibited more efficient than mono oxide, where these oxides act as active sites for interaction with cyclic sulfur compounds [2]. Nezal et al., (2015) studied activated carbon loaded with aluminum oxide; the highest removal of DBT of 98% for model fuels with sulfur content 250 ppm and 30% for real fuels at high concentration. Also Ma (2007) used real jet fuel with sulfur content 717 ppm to obtain 61.2% of removal [16]. The decrease in the removal can be attributed to the presence of other hydrocarbons affecting the selectivity.

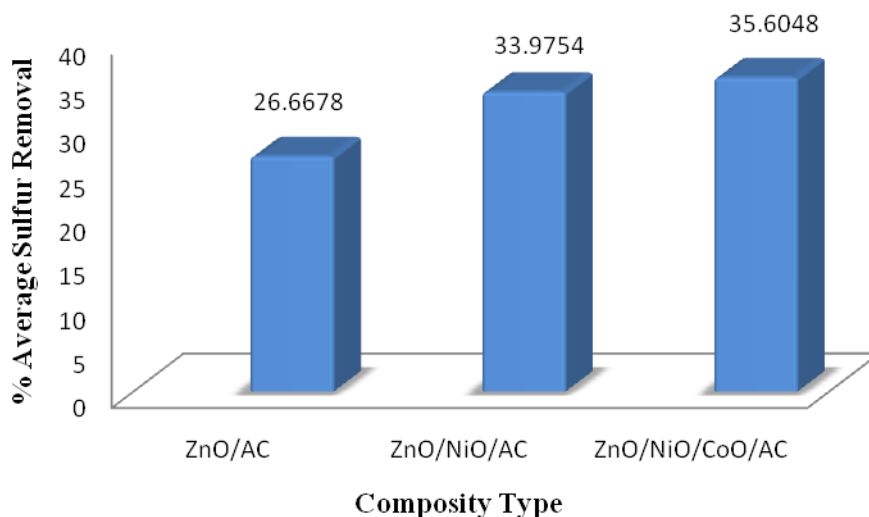


Fig 10 Mean Effect of Composite Type on Sulfur Removal

The contribution on CoO in the composite in addition to the oxidation process using O_2 to convert cyclic sulfur compounds to corresponding sulfone, improves the interaction with sulfur compound and the surface. To explain how sulfone adsorbs on the surface of the adsorbents, the concept of the Gibb's free energy of adsorption will be employed. The free energy ΔG_{abs} as equation (4) [26].

$$\Delta G_{abs} = \Delta G_c + \Delta G_{hb} + \Delta G_{id} \quad \dots (4)$$

ΔG_c is related to surface metal cations (Zn^{+2} , Ni^{+2} and Co^{+2}) bonds formed by sharing of electrons between metal ions and sulfur atom. ΔG_{hb} refers to the hydrogen-bonding, between a single couple of electron of sulfur atom and a hydrogen atom that is bonded to oxygen. ΔG_{id} is for ion-dipole interactions, where ion-dipole interactions consist of interactions between a charged ion and a polarsulfone.

Activated carbon has various functional groups at its surface. The presence of the oxygen atoms on the sulfur compounds makes them polar molecules easy to interact with the functional groups on the activated carbon. Figure 11 shows how sulfone interacts with loaded activated carbon surface.

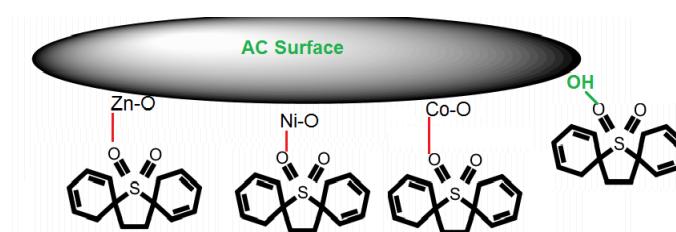


Fig 11: π - Interactions of DBT molecules with the adsorbents.

Effect of Amount of Composite

The effect of amount of composite on ODS process was investigated. Increasing the amount of composite improved the sulfur removal performance as a result to increase of active surface area for adsorption of the oxidized sulfur compounds. Figure 12 shows the effect of amount of composite on sulfur removal.

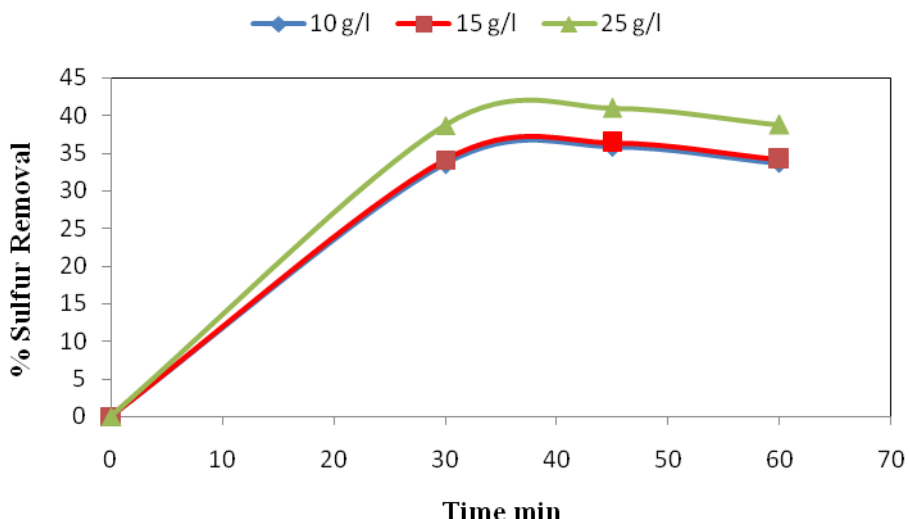


Fig 12: Effect of Composite Amount on Sulfur Removal

Effect of Oxygen Flow Rate

In ODS process in SBCR, oxygen gas is used as the oxidant; therefore, the influence of the oxygen flow rate on sulfur removal was studied. The results, shown in Figure 13, indicate that the rate of ODS process is increased with increasing oxygen flow rate, and a higher extent of sulfur removal was achieved with oxygen flow rate of 19.0476 l/min. This increase is due to the increase in the gas holdup as the oxygen gas velocity increases. As a result the volumetric gas transfer coefficient is increased also. The volumetric gas mass transfer coefficient is a linear relationship with superficial gas velocity. K_{La} depends on the assumption that gas holdup is directly proportional to superficial gas velocity [35]. Since the conversion of sulfur compounds to the corresponding sulfones is increased by increasing oxygen gas, hence, is more adsorbed than sulfides on the surface of metal oxide loaded AC where the hydrophobic nature of the parent AC is modified to hydrophilic by this loading to enhance the selectivity[23]. Figure 14 shows the relationship between gas holdup and gas velocity in the present work.

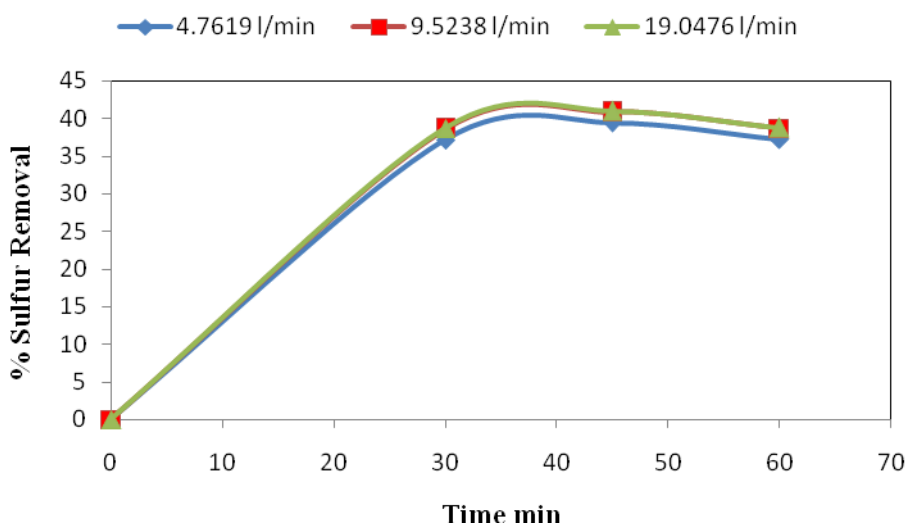


Fig 13: Effect of Oxygen Gas Flow Rate on Sulfur Removal

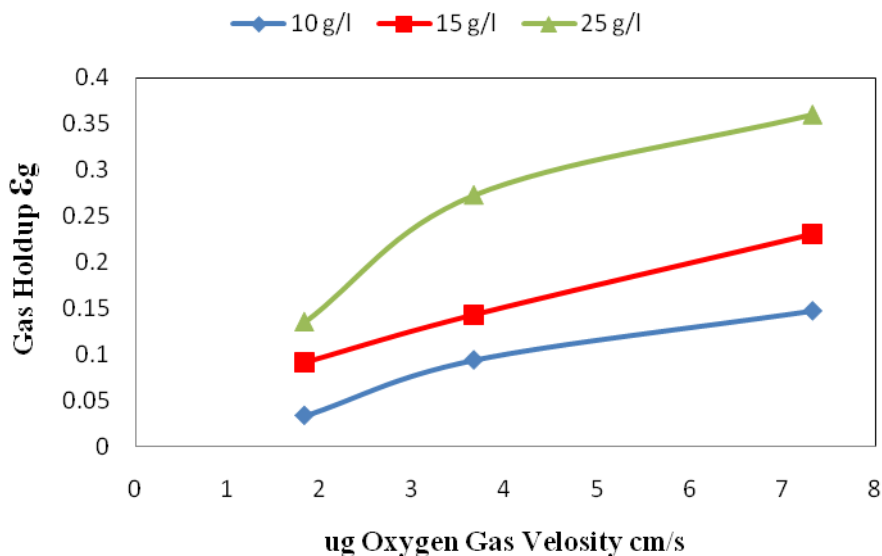


Fig 14: Relationship between Gas Hold up and Gas Velocity

Effect of Time

The effect of time on the removal of sulfur compound is shown in Figure 15. As the time of ODS increases from 30 to 45 min, the sulfur removal increased due to the increased amount of sulfur compounds removed by the hydroperoxide that converts sulfides to sulfones as the time of ODS process proceeds. But above 45 min, the sulfur removal was decreased, which can be explained by reaching the maximum capacity for composites and equilibrium. In the previous studies, the time for maximum removal was contrasted ranging from 1 to 3 hours depending on many factors like; the initial sulfur content, type of fuel (synthetic model or real fuel), the type of metal oxide composite, the technique (batch, semi batch or continuous) and the type of the oxidant if the oxidation process is employed and not adsorption only, where most of the studies adopted the adsorption process without oxidation..

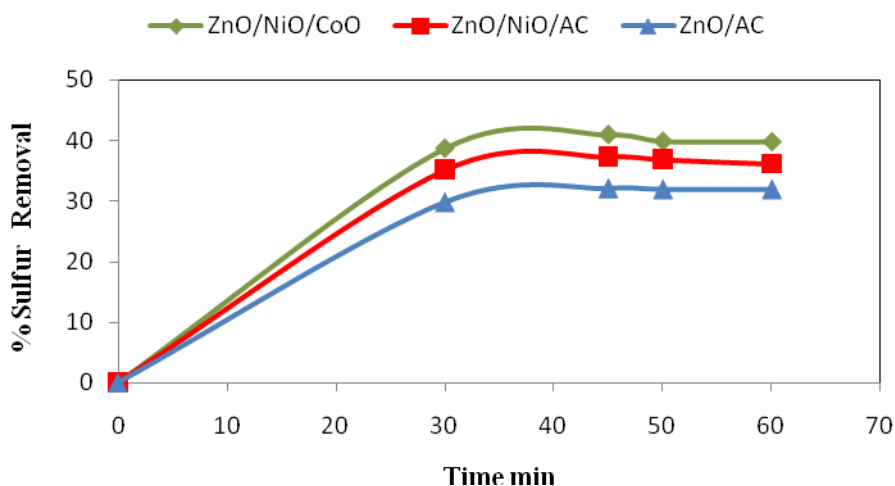


Fig 15: Effect of Time on Sulfur Removal

Figure 16 show the comparison between kerosene fuel and model fuel, it is observed that the behavior for desulfurization kerosene fuel follows the trend for the model fuel. These results reveals that the DBT is the predominate sulfur compound and is being subjected to the treatment. Also, it can be deduced that a time of about 50 min is quite satisfactory for completeness. Small differences can be attributed to the experimental errors.

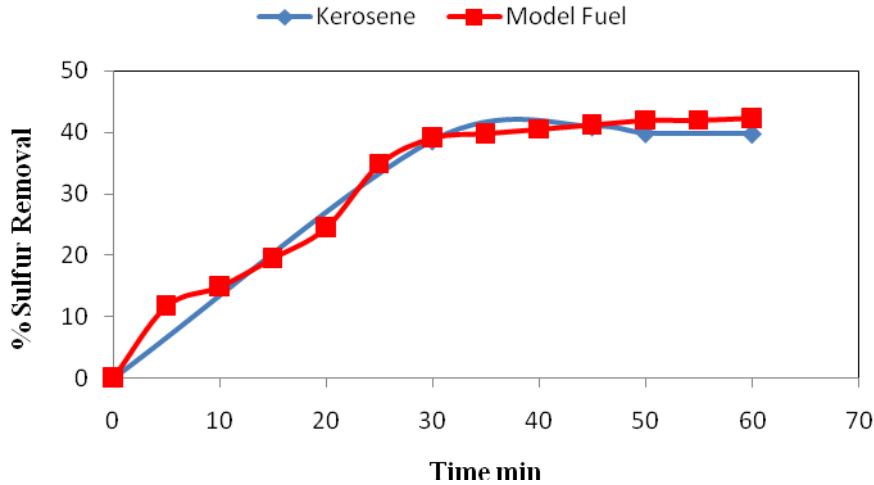


Fig 16: The Comparison between Kerosene and Model Fuels

Kinetic Study

The design of experiment does not tell anything about the kinetics of the reaction. The kinetics of oxidation in batch experiment for model fuel with ZnO/AC, kerosene fuel and model fuel with three type of composite was studied. In the present work the kinetic model was examined by pseudo-first order and pseudo second order kinetic rate equation to find the best kinetic model by comparison between correlation coefficient R². Equations (5) represent the pseudo first order kinetic and equation (6) represents pseudo second order kinetic.

$$\ln \frac{C_0}{C_t} = kt \dots (5)$$

$$\frac{1}{C_t} = \frac{1}{C_0} + kt \dots (6)$$

i. Semi-batch SBC Kinetics for Kerosene Fuel

The kinetics of oxidation of kerosene with sulfur content 2850 ppm was studied with different type of composite in SBC. Figure (17) and Figure (15) show the effect of time on the concentration and percent removal of sulfur for the three types of composites, it is observed that the concentration of DBT after 45 min was increased.

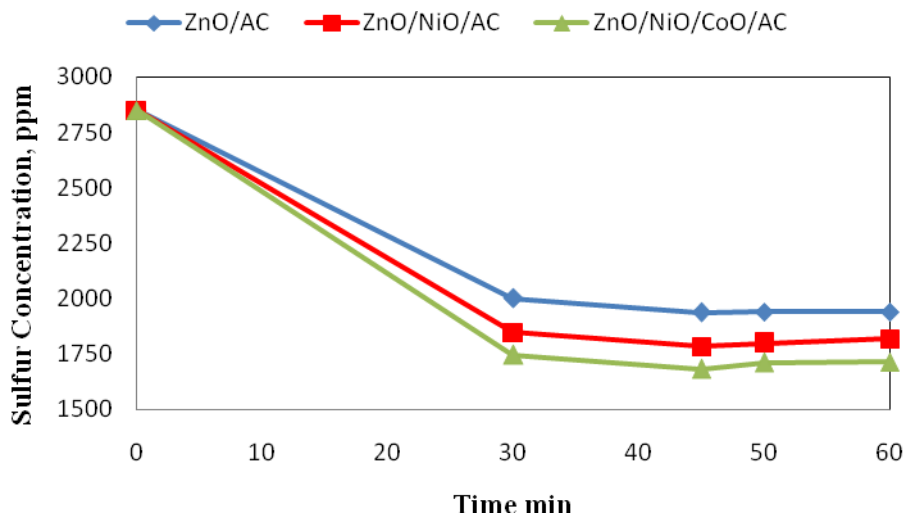


Fig 17: Effect of Time on the Sulfur Concentration

Table 6 list the comparison between two kinetic models, since pseudo second order kinetic show the good fit than the pseudo first order kinetics.

Table 6: The Comparison between two Kinetic Models in Semi Batch SBC for Kerosene Fuel

| Composite Type | Pseudo First Order | | Pseudo Second Order | |
|----------------|---------------------|----------------|---------------------|----------------|
| | k min ⁻¹ | R ² | k g/mg.min | R ² |
| ZnO/AC | 0.0078 | 0.8025 | 3 E-6 | 0.8448 |
| ZnO/NiO/AC | 0.0093 | 0.768 | 3.5 E-6 | 0.8115 |
| ZnO/NiO/CoO/AC | 0.0105 | 0.7651 | 4 E-6 | 0.8092 |

ii. **Semi-Batch SBC Kinetics for Model Fuel**

The kinetics of oxidation of DBT dissolved in n-nonane with sulfur content 2250 ppm as model fuel was studied with different type of composite. The reaction is a three phase heterogeneous kind, the organic phase contains the reactant DBT, n-nonane the aqueous phase contains the oxidant sulfone and the composite makes the solid phase.

Kinetic removal of DBT from model fuel in presence of varies type of oxides loaded on activated carbon, were observed by measuring the DBT concentration at different time until the equilibrium reach. Figure (18) and Figure (19) show the effect of time on the DBT concentration and percent DBT removal for the three types of composites, it is observed that the concentration of DBT after 55 min was increased. This observation coincides with kerosene fuel; the mean effect of sulfur removal was decreased after 45 min. The tri composite in model fuels have the highest present removal of 43.4 compared to the mono and di composite of 36.64 and 40.56 respectively. This indicated that equilibrium time was reached and /or the model fuel, or other hydrocarbons in case of real fuel, is being adsorbed causing a decrease in the total weight or volume.

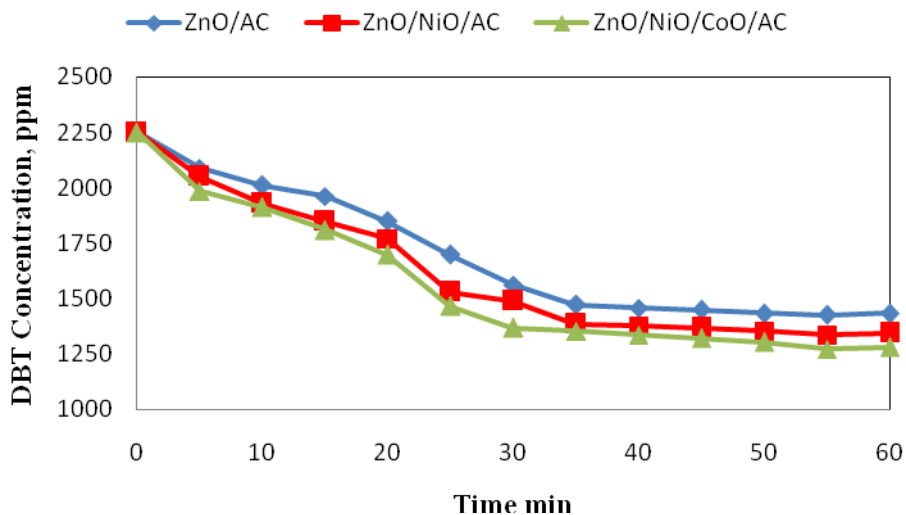


Fig 18: Effect of Time on the DBT Concentration

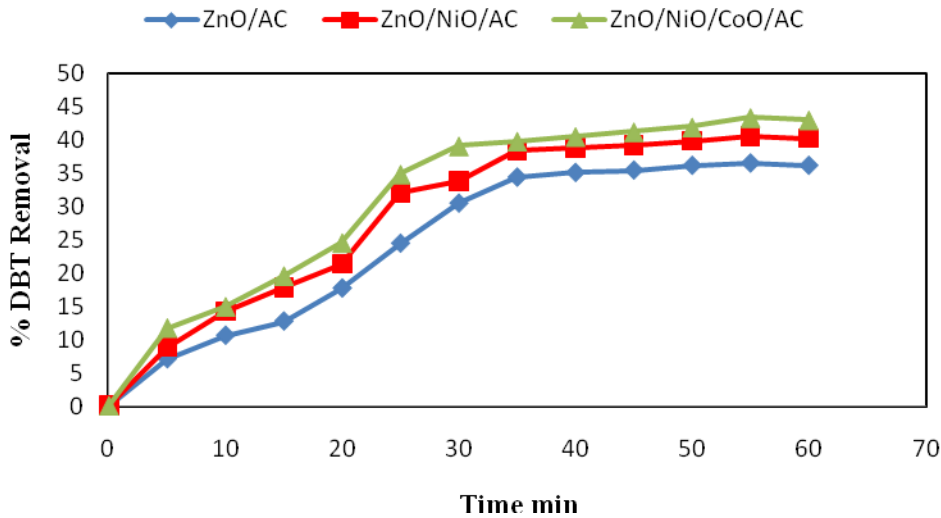


Fig 19: Effect of Time on the DBT Removal

Table 7 list the comparison between two kinetic models, since pseudo second order kinetic show the good fit than the pseudo first order kinetics.

Table 7: The Comparison between two Kinetic Models in Semi Batch SBC for Model Fuel

| Composite Type | Pseudo First Order | | Pseudo Second Order | |
|----------------|----------------------------------|----------------|---------------------|----------------|
| | k ₁ min ⁻¹ | R ² | k g/mg.min | R ² |
| ZnO/AC | 0.0099 | 0.9241 | 5 E-6 | 0.9419 |
| ZnO/NiO/AC | 0.0114 | 0.8867 | 5.6 E-6 | 0.9343 |
| ZnO/NiO/CoO/AC | 0.0125 | 0.8549 | 6 E-6 | 0.9227 |

Pore Diffusion

The effect of internal mass transfer for the ODS of DBT using oxygen and three type of composites by calculating the Thiele modulus (M_T) as equation (7) [36].

$$M_T = L \sqrt{\frac{(n+1)K_{eff}C_{DBT}^{n-1}}{2D_{eff}}} \dots (7)$$

For a second order equation the equation (7) reduced to equation (8):

$$M_T = L \sqrt{\frac{3K_{eff}.C_{DBT}}{2D_{eff}}} \dots (8)$$

Where the effective diffusivity can be evaluated from equation (9):

$$D_{eff} = \frac{D_{AB}\epsilon_p}{\tau_p} \dots (9)$$

In this work, $L = \frac{R}{3}$ for sphere particles (R is the radius of particle from the AFM results, are 52.36 nm, 59 nm and 52.36 nm for mono, di and tri composites respectively), for activated carbon the porosity ϵ_p are measured as 0.89, while, the tortuosity τ_p for activated carbon process range is 1-12 The value of the tortuosity τ_p can be chosen as 3.5, since this value was chosen by many researchers in the literature[37]. The tortuosity τ_p can be mathematically expressed as the equation (10) [38].

$$\tau_p = \frac{\text{Actual distance molecule travels from a to b}}{\text{Shortest distance between a and b}} \dots (10)$$

The molecular diffusion coefficient of the oxygen in n-Nonane(D_{AB}) is 0.0495 cm²/s at 67°C was measured by Cummings 1955 and by extrapolated is 0.05789 cm²/s at 25°C [39].

Table 7: Thiele Modulus Calculation in Semi Batch SBC

| Composite Type | Kerosene | | |
|----------------|------------|-----------------|-------------|
| | L cm | K_{eff} /mg.s | M_T |
| ZnO/AC | 1.7453E-06 | 5.00E-08 | 1.73376E-07 |
| ZnO/NiO/AC | 1.9668E-06 | 5.83E-08 | 1.99364E-07 |
| ZnO/NiO/CoO/AC | 1.7453E-06 | 7.50E-08 | 1.97887E-07 |
| | Model Fuel | | |
| ZnO/AC | 1.7453E-06 | 8.33E-08 | 1.92019E-07 |
| ZnO/NiO/AC | 1.9668E-06 | 9.17E-08 | 2.296E-07 |
| ZnO/NiO/CoO/AC | 1.7453E-06 | 1.00E-07 | 1.98803E-07 |

The calculated Thiele modulus values for the composites are listed in Table 7. It can be seen that, all values of Thiele modulus (M_T) are less than 0.4, and its indication is that the effect of internal mass transfer on the overall reaction rate can be neglected and these results could be attributed to the high pore volume and the small particle size that made pore diffusion resistance very small.

CONCLUSIONS

The prepared composite of ZnO/NiO/CoO/AC is found the best one with average sulfur removal of about 36% for kerosene. When increasing the amount of composite to 25 g/l and the oxygen gas flow rate the sulfur removal increases. The sulfur removal increases with increasing the time of reaction from 30 to 45 min reached the maximum after 45 min for kerosene fuel. For the kinetic study, it was observed that the equilibrium occurs at 55 min for model fuel. Optimization of the factors according to Taguchi method revealed the ZnO/NiO/CoO/AC composite was the most influential factor on the average percent sulfur removal in the present system and the oxygen gas flow rate has a less effect with comparing to other factors in present system. The best factors conditions according to Taguchi method from the present work are ZnO/NiO/CoO/AC composite, composite amount 25 g/l, oxygen gas flow rate 19.0476 l/min and time of reaction 45 min. The reaction is kinetically described by pseudo second order reaction. The Thiele modulus (M_T) calculated for model fuel is less than 0.4, and it refers to that the effect of internal mass transfer on the overall reaction rate is not significant.

ACKNOWLEDGMENT

Ministry of oil/ Petroleum Research and Development Center is highly acknowledged for the financial support. Also, our thankfulness goes to the Iraqi-German Labs / College of Science for measurements.

Nomenclature

| Symbol | Definition |
|-----------|--------------------------------------|
| C_{DBT} | Concentration of dibenzothiophene |
| D_{eff} | Effective Diffusivity Coefficient |
| D_{AB} | Molecular Diffusion Coefficient |
| d_o | Hole diameter of the distributor |
| H_o | Static Height without gas sparger |
| H_d | Height of Slurry Dispersion |
| K | Rate Constant of the Reaction |
| K_{La} | Volumetric mass transfer coefficient |
| K_{eff} | Effective rate constant |
| N | order of the reaction |

L characteristic length of the catalyst particles

Greek Letters

ϵ_p Porosity of the composite particles

ϵ_g Gas hold up

ρ Density

τ_p Tortuosity of the composite pores

Θ Scattering or Bragg angle

Σ Surface tension

Dimensionless Numbers

M_T Thiele modulus

REFERENCES

- [1] S. Murata, K. Murata, K. Kidena, and M. Nomura, "A novel oxidative desulfurization system for diesel fuels with molecular oxygen in the presence of cobalt catalysts and aldehydes," *Energy and Fuels*, 2004.
- [2] M. N. Alhooshani, Khalid R., Abdullah A. , Saleh, Tawfik A. , Siddiqui, "Methods for preparing composites of activated carbon / zinc oxide and activated carbon / zinc oxide / nickel oxide for desulfurization of fuels," 20150148581 A1, 2015.
- [3] C. Zuber, C. Hochenauer, and T. Kienberger, "Test of a hydrodesulfurization catalyst in a biomass tar removal process with catalytic steam reforming," *Appl. Catal. B Environ.*, vol. 156–157, pp. 62–71, 2014.
- [4] D. Sullivan, "The Role of the Merox Process in the Era of Ultra Low Sulfur Transportation Fuels," in *Transportation*, 2004, pp. 1–11.
- [5] H. Rang, J. Kann, and V. Oja, "Advances in desulfurization research of liquid fuel," *Oil Shale*, 2006.
- [6] R. Sundararaman, X. Ma, and C. Song, "Oxidative desulfurization of jet and diesel fuels using hydroperoxide generated in situ by catalytic air oxidation," *Ind. Eng. Chem. Res.*, vol. 49, no. 12, pp. 5561–5568, 2010.
- [7] A. T. Nawaf, S. A. Gheni, A. T. Jarullah, and I. M. Mujtaba, "Optimal Design of a Trickle Bed Reactor for Light Fuel Oxidative Desulfurization Based on Experiments and Modeling," *Energy & Fuels*, vol. 29, no. 5, pp. 3366–3376, 2015.
- [8] T. V. Rao, B. Sain, S. Kafola, B. R. Nautiyal, K. Sharma, S. M. Nanoti, M. O. Garg, and Y. K. Sharma, "Oxidative Desulfurization of HDS Diesel Using the Aldehyde / Molecular Oxygen Oxidation System Oxidative Desulfurization of HDS Diesel Using the Aldehyde / Molecular Oxygen Oxidation System," vol. 50, no. 13, pp. 3420–3424, 2007.
- [9] D. Liu, "Catalytic Oxidative Desulfurization of a Model Diesel," Louisiana State University, 2010.
- [10] F. M. Al-Shahrani, T. Xiao, H. Shi, and Malcolm L. H. Green, "Hydrocarbon Recovery from Sulfones Formed by Oxidative Desulfurization Process," US 8663459B2, 2014.
- [11] B. Wang, J. Zhu, and H. Ma, "Desulfurization from thiophene by SO_4^{2-}/ZrO_2 catalytic oxidation at room temperature and atmospheric pressure," *J. Hazard. Mater.*, vol. 164, pp. 256–264, 2009.
- [12] H. X. Zhang, J. J. Gao, H. Meng, Y. Z. Lu, and C. X. Li, "Catalytic Oxidative Desulfurization of Fuel by H_2O_2 In Situ Produced via Oxidation of 2-Propanol," *Ind. Eng. Chem. Res.*, vol. 51, pp. 4868–4874, 2012.
- [13] L. Gao, Q. Xue, Y. Liu, and Y. Lu, "Base-free catalytic aerobic oxidation of mercaptans for gasoline sweetening over HTLcs-derived CuZnAl catalyst," *AIChE J.*, 2009.
- [14] W. H. C. Amir Attar, "Technical review," *Ind. Eng. Prod. Res. Dev.*, vol. 17, no. 2, pp. 102–109, 1978.
- [15] J. H. Sherman, "Methods of Improving the Quality of Diesel Fuel," 0015339 A1, 2001.
- [16] X. Ma, A. Zhou, and C. Song, "A novel method for oxidative desulfurization of liquid hydrocarbon fuels based on catalytic oxidation using molecular oxygen coupled with selective adsorption," *Catal. Today*, 2007.
- [17] Ahmad Imtiaz, A. Waqas, and I. Muhammad, "Desulfurization of Liquid Fuels Using Air Assisted Performic Acid Oxidation And Emulsion Catalyst," *Chinese J. Catal.*, vol. 34, no. 2, pp. 1839–1847, 2013.
- [18] J. Wang, Q. Guo, C. Zhang, and K. Li, "One-pot extractive and oxidative desulfurization of liquid fuels with molecular oxygen in ionic liquids," *RSC Adv.*, vol. 4, no. 104, pp. 59885–59889, 2014.
- [19] J. Ding and R. Wang, "Oxidation Of Dibenzothiophene Using Oxygen And A Copper Phosphotungstate Catalyst For Deep Desulfurization Of Fuels," vol. 57, no. 3, pp. 291–294, 2015.
- [20] N. Kantarci, F. Borak, and K. O. Ulgen, "Bubble column reactors," *Process Biochem.*, vol. 40, no. 7, pp. 2263–2283, 2005.
- [21] E. Ahumada, H. Lizama, F. Orellana, C. Suárez, A. Huidobro, A. Sepúlveda-Escribano, and F. Rodríguez-Reinoso, "Catalytic oxidation of Fe(II) by activated carbon in the presence of oxygen. Effect of the

- surface oxidation degree on the catalytic activity," *Carbon N. Y.*, vol. 40, no. 15, pp. 2827–2834, 2002.
- [22] K. R. Alhooshani, 1Mohammad Nahid Siddiqui, T. A. Saleh, and M. A. Gondal, "Adsorptive Desulfurization of Model Fuel Oil using Novel Metal Oxide," *Prepr. Pap.-Am. Chem. Soc., Div. Energy Fuels Prepr.*, vol. 58, no. 1, 2013.
- [23] M. Seredych and T. J. Badosz, "Adsorption of dibenzothiophenes on activated carbons with Ag, Co and Ni deposited on their surfaces," *Energy and Fuels*, vol. 23, pp. 3737–3744, 2009.
- [24] E. S. Moosavi, S. A. Dastgheib, and R. Karimzadeh, "Adsorption of thiophenic compounds from model diesel fuel using copper and nickel impregnated activated carbons," *Energies*, vol. 5, no. 10, pp. 4233–4250, 2012.
- [25] M. K. Nazal, M. Khaled, M. A. Atieh, I. H. Aljundi, G. A. Oweimreen, and A. M. Abulkibash, "The nature and kinetics of the adsorption of dibenzothiophene in model diesel fuel on carbonaceous materials loaded with aluminum oxide particles," *Arab. J. Chem.*, 2015.
- [26] T. Chen, M. L. Agripa, M. Lu, and M. L. P. Dalida, "Adsorption of Sulfur Compounds from Diesel with Ion-Impregnated Activated Carbons," *Energy & Fuels*, 2016.
- [27] T. Jirsak, J. Dvorak, and J. A. Rodriguez, "Chemistry of Thiophene on ZnO, S/ZnO, and Cs/ZnO Surfaces: Effects of Cesium on Desulfurization Processes," *J. Phys. Chem. B*, vol. 103, no. 26, pp. 5550–5559, 1999.
- [28] X. Meng, H. Huang, H. Weng, and L. Shi, "Ni/ZnO-based Adsorbents Supported on Al₂O₃, SiO₂, TiO₂, ZrO₂: A Comparison for Desulfurization of Model Gasoline by Reactive Adsorption," *Bull. Korean Chem. Soc.*, vol. 33, no. 10, pp. 3213–3217, 2012.
- [29] A. Kong, Y. Wei, and Y. Li, "Reactive adsorption desulfurization over a Ni/ZnO adsorbent prepared by homogeneous precipitation," *Front. Chem. Sci. Eng.*, vol. 7, no. 2, pp. 170–176, 2013.
- [30] N. M. Deraz, A. Alarifi, and S. A. Shaban, "Removal of sulfur from commercial kerosene using nanocrystalline NiFe₂O₄ based sorbents," *J. Saudi Chem. Soc.*, vol. 14, no. 4, pp. 357–362, 2010.
- [31] R. N. Matti, "Influence of the Geometric Variables of a Bubble Column on Gas Hold-up and Bubble Characteristics," *University of Technology*, 2006.
- [32] Mathesonrigas, "Basic Flowmeter Principles," *Flow Measurement & Control*, pp. 351–354.
- [33] J. Chaichanawong, T. Yamamoto, T. Ohmori, and A. Endo, "Adsorptive desulfurization of bioethanol using activated carbon loaded with zinc oxide," *Chem. Eng. J.*, vol. 165, no. 1, pp. 218–224, 2010.
- [34] S. P. Hernandez, M. Chiappero, N. Russo, and D. Fino, "A novel ZnO-based adsorbent for biogas purification in H₂ production systems," *Chem. Eng. J.*, vol. 176–177, pp. 272–279, 2011.
- [35] A. Kommareddy and G. Anderson, "Analysis of currents and mixing in a modified bubble column reactor," vol. 300, no. 4, pp. 4105–4114, 2004.
- [36] O. Levenspiel, *Chemical Reaction Engineering*, Third Edit. John Wiley & Sons, Inc., 1999.
- [37] R. Leyva-Ramos and C. J. Geankoplis, "Diffusion in Liquid-Filled Pores of Activated Carbon. I. Pore Volume Diffusion," *Can. J. Chem. Eng.*, vol. 72, pp. 262–271, 1994.
- [38] H. S. Fogler, *Elements of Chenzicn 1 Reaction Engineering*, Fourth Edi. Prentice-Hall International Inc., New Jersey, 2006.
- [39] M. J. Tang and M. Kalberer, "Supplement of Compilation and evaluation of gas phase diffusion coefficients of reactive trace gases in the atmosphere : Volume 2 . Diffusivities of organic compounds , pressure-normalised mean free paths , and average Knudsen numbers for gas uptake calcu," *Atmos. Chem. Phys.*, vol. 15, pp. 5585–5598, 2015.